Mononuclear Molybdenum(IV) Complexes with Two Multiply Bonded Chalcogen Ligands in Trans Configuration and Chelating Biphosphine Ligands

F. Albert Cotton* and Günter Schmid

Department of Chemistry, Texas A&M University, College Station, Texas 77843-3255

Received August 30, 1996[⊗]

A series of molybdenum(IV) complexes of the type *trans*-Mo(Q)(Q′)(P⌒P)$_2$ has been prepared where Q and Q′ are chalcogen ligands (O, S, Se, Te) and P⌒P is either *cis*-1,2-bis(diphenylphosphino)ethylene (dppee) or 1,2-bis(diphenylphosphino)ethane (dppe). X-ray crystallographic studies were carried out to investigate how the Mo−Q distance is influenced by the mutually competitive $d_\pi-p_\pi$ interactions between the p_x and p_y orbitals of the chalcogen ligands and the d_{xz} and d_{yz} orbitals of the molybdenum center. *trans*-Mo(O)$_2$(dppee)$_2$ (**1**) has been prepared by the hydrolysis and deprotonation reaction of [Mo(O)(Cl)(dppee)$_2$]Cl with NaOH in methanol. The compounds where Q represents the heavier chalcogens (S, Se, Te) have been prepared by the reaction between *trans*-Mo(N$_2$)$_2$(P⌒P)$_2$ and a chalcogen source: *trans*-Mo(S)$_2$(dppee)$_2$ (**2**), BzS$_3$Bz (dibenzyl trisulfide); *trans*-Mo(Se)$_2$(dppee)$_2$ (**3**), elemental Se; *trans*-Mo(Te)$_2$(dppee)$_2$ (**4**), TePEt$_3$ (Et = ethyl); *trans*-Mo(S)$_2$(dppe)$_2$ (**5**), BzS$_3$Bz; *trans*-Mo(Se)$_2$(dppe)$_2$ (**6**), Se. *trans*-Mo(O)(S)(dppee)$_2$ (**7**) was obtained from the reaction of MoCl$_3$(THF)$_3$ (THF = tetrahydrofuran), dppee, and NaHS in a mixture of THF and methanol. The attempted preparation of **7** by the reaction of SO$_2$ and *trans*-Mo(N$_2$)$_2$(dppee)$_2$ yielded Mo(SO$_2$)$_2$(dppee)$_2$ (**8**). **1** crystallizes in the monoclinic space group $P2_1/c$ (No. 14, $Z = 2$) with $a = 11.1340(15)$ Å, $b = 18.435(2)$ Å, $c = 12.515(2)$ Å, and $\beta = 110.999(9)°$; **2** crystallizes in the triclinic space group $P\bar{1}$ (No. 2, $Z = 1$) with $a = 10.102(4)$ Å, $b = 10.722(4)$ Å, $c = 12.195(3)$ Å, $\alpha = 100.95(3)°$, $\beta = 95.04(4)°$, and $\gamma = 117.81(2)°$; **3** crystallizes in the monoclinic space group $P2_1/c$ (No. 14, $Z = 2$) with $a = 11.186(5)$ Å, $b = 18.005(8)$ Å, $c = 12.761(9)$ Å, and $\beta = 110.35(4)°$; **4** crystallizes in the triclinic space group $P\bar{1}$ (No. 2, $Z = 2$) with $a = 12.681(4)$ Å, $b = 19.280(5)$ Å, $c = 10.454(3)$ Å, $\alpha = 104.60(2)°$, $\beta = 111.61(2)°$, and $\gamma = 75.12(2)°$; **5** crystallizes in the monoclinic space group $C2/c$ (No. 15, $Z = 8$) with $a = 49.515(7)$ Å, $b = 10.9286(12)$ Å, $c = 18.203(3)$ Å, and $\beta = 98.306(12)°$; **6** crystallizes in the monoclinic space group $C2/c$ (No. 15, $Z = 8$) with $a = 49.566(9)$ Å, $b = 10.9765(15)$ Å, $c = 18.282(3)$ Å, and $\beta = 98.541(13)°$; **7** crystallizes in the triclinic space group $P\bar{1}$ (No. 2, $Z = 1$) with $a = 10.040(1)$ Å, $b = 10.563(1)$ Å, $c = 12.162(2)$ Å, $\alpha = 75.30(1)°$, $\beta = 85.93(1)°$, and $\gamma = 63.21(1)°$; **8** crystallizes in the monoclinic space group $C2/c$ (No. 15, $Z = 4$) with $a = 21.534(6)$ Å, $b = 12.4271(13)$ Å, $c = 19.550(5)$ Å, and $\beta = 118.480(14)°$. The UV/vis and the $^{31}P\{^1H\}$ NMR data for compounds **1**−**7** are also reported and discussed.

Introduction

Complexes with multiply bonded ligands are of great interest in various aspects of chemistry.[1] For instance, molybdenum compounds have been studied as models for enzymes. Though molybdenum forms, by far, the largest number of complexes containing metal−ligand multiple bonds among the transition metals, mononuclear species, especially those with more than one multiply bonded ligand, are rather rare or have the cis configuration. The strong tendency of the chalcogen ligand to form bridges accounts for the larger number of molybdenum clusters and polyanions.[2a]

In this paper, we report the syntheses and structural and spectroscopic studies of octahedral mononuclear molybdenum compounds having chelating phosphino ligands in the equatorial positions and competing chalcogen ligands at the apices. The σ bonding framework is mostly formed by the metal $d_{x^2-y^2}$ and d_{z^2} orbitals. In our d^2 system, the filled p_x and p_y lone pair orbitals of the chalcogen ligand can form up to two π interactions with the d_{xz} and d_{yz} orbitals and formally a maximum bond order of 3 is possible (Figure 1). We call the reader's attention to another recent, major contribution to the study of this class of compounds by Rabinovich and Parkin.[2b]

The Mo═Q bond distances determined by X-ray crystallography will be discussed in this framework. The electronic structure of d^2 complexes with a single double-bonded chalcogen ligand was successfully predicted by ligand field theory.[1] However, the electronic structure of complexes of the type discussed here is strongly dependent on the level of the theory used for the calculations. Detailed discussion and comparison with the measured electronic spectra are found in a preceding paper.[3]

Experimental Section

General Procedures. All preparations were carried out under an atmosphere of N_2 using standard Schlenk techniques and a vacuum line. All nonhalogenated solvents were freshly distilled from Na/K benzophenone ketyl prior to use. Methanol was dried over magnesium. Dichloromethane was freshly distilled from P_2O_5. Solutions were transferred *via* stainless steel cannulae or syringes through rubber septa. UV/vis spectra were recorded on a Varian Cary 17D spectrometer. EDX analyses were carried out with the DSM 962 electron microscope (Zeiss) at the University of Ulm (Germany). ^{31}P NMR data were recorded on a Varian XL200 broad-band spectrometer with H_3PO_4 in D_2O as external references. Fast atom bombardment (FAB) mass spectra (Xe

* Author to whom correspondence should be addressed.

[⊗] Abstract published in *Advance ACS Abstracts,* May 1, 1997.

(1) Nugent, W. A.; Mayer, J. M. *Metal-Ligand Multiple Bonds*; Wiley: New York, 1988.

(2) (a) Cotton, F. A.; Wilkinson, G. *Advanced Inorganic Chemistry,* 5th ed.; Wiley: New York, 1982; p 804. (b) Rabinovich, D.; Parkin, G. *Inorg. Chem.* **1995**, *34*, 6841.

(3) Cotton, F. A.; Feng, X. *Inorg. Chem.* **1996**, *35*, 4921.

S0020-1669(96)01071-3 CCC: $14.00

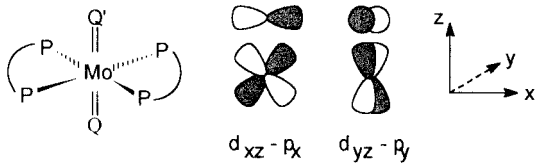

Figure 1. Complexes of the type $Mo(Q)_2(P^\frown P)_2$ with metal−ligand $d_\pi-p_\pi$ interactions of the Mo d^2 system and the lone pair orbitals on the chalcogen ligand. The coordinate system was defined as depicted.

ions, 8 keV) were measured on a VG Analytical (Manchester, U.K.) 70-S high-resolution, double-focusing, magnetic sector mass spectrometer (solvent CH_2Cl_2, matrix nitrobenzyl alcohol or nitrophenyl octyl ether). *trans*-$Mo(N_2)_2$(dppee)$_2$ (dppee = *cis*-1,2-bis(diphenylphosphino)ethylene)[4] and *trans*-$Mo(N_2)_2$(dppe)$_2$ (dppe = 1,2-bis(diphenylphosphino)ethane)[5] were prepared according to literature procedures. The synthesis and structural characterization of [*trans*-Mo(O)(Cl)(dppee)$_2$]Cl will be reported in a separate paper.[6] The phosphines dppee and dppe (Strem) were used as purchased. SO_2 was bought in a lecture bottle (Aldrich).

Preparation of *trans*-Mo(O)$_2$(dppee)$_2$ (1). a. Compound **1** was prepared by the reaction of *trans*-[Mo(O)(Cl)(dppee)$_2$]Cl with air and moisture in methanol in the presence of Li_2S acting as a base: A solution of 20 mg of Li_2S in 15 mL of methanol was added dropwise to 196 mg (0.2 mmol) of *trans*-[Mo(O)(Cl)(dppee)$_2$]Cl in 15 mL of methanol. A small amount of a brownish precipitate was formed, which was filtered off and discarded. The filtrate was allowed to evaporate slowly, in air, by covering the beaker with filter paper. After a few days, pale-yellow cube-shaped crystals of $Mo(O)_2(dppee)_2 \cdot 2CH_3OH$ were collected (65 mg, 30%).

b. 1 was also obtained by titrating a solution of 238 mg (0.25 mmol) of *trans*-[Mo(O)(Cl)(dppee)$_2$]Cl in methanol with a solution of 12 mg of NaOH in 15 mL of methanol until a pH of 8 was reached. During the addition, the color of the reaction mixture changed from red-purple to yellow-orange. The solvent was distilled and the yellow residue washed with small amounts of water and methanol. The yield was almost quantitative. The FAB mass spectrum of the residue showed the parent ion $(M + H)^+$ and only fragments which are expected upon decomposition of **1**. The purity was further established by ^{31}P NMR.

***trans*-Mo(O)$_2$(dppee)$_2$ (1):** mp *ca*. 160 °C dec; $^{31}P\{^1H\}$ NMR (81 MHz, CH_2Cl_2, room temperature) $\delta = 49.3$ ppm (singlet). The presence of the heavier elements Mo and P was confirmed by EDX (Kα, Lα). FAB-DP$^+$-MS (nitrobenzyl alcohol as matrix, CH_2Cl_2) from crystals (a) or powder (b): $m/z = 923$ ($(M + H)^+$, relative intensity 12%), 527 ($(M -$ dppee$)^+$, 12), 397 ($(dppee)^+$, 2). The calculated isotopic pattern at $m/z = 923$ is in good agreement with the recorded values. UV/vis (methanol, nm): 438 (sh, 25), 373 (sh, 100).

Preparation of *trans*-Mo(S)$_2$(dppee)$_2$ (2). An orange solution of 250 mg of *trans*-$Mo(N_2)_2$(dppee)$_2$ (0.26 mmol) and 170 mg of dibenzyl trisulfide (0.61 mmol) in 35 mL of toluene was refluxed for 2 h. After the mixture was cooled to room temperature, the brown-orange precipitate was filtered off and washed three times with 15 mL of diethyl ether (yield 155 mg, 62%). After the raw product was dissolved in CH_2Cl_2 and the solution was layered with THF and subsequently with hexanes, up to 1.5 mm large brown crystals of **2** were formed over a period of 3 weeks. Smaller crystals of **2** could also be obtained by warming a solution of 180 mg of *trans*-$Mo(N_2)_2$(dppee)$_2$ (0.19 mmol) and 105 mg of dibenzyl trisulfide (0.38 mmol) in 60 mL of THF without stirring (yield 90 mg, 50%).

***trans*-Mo(S)$_2$(dppee)$_2$ (2):** mp = 256−258 °C dec; $^{31}P\{^1H\}$ NMR (81 MHz, CH_2Cl_2, room temperature) $\delta = 50.5$ ppm (singlet). The presence of the heavier elements Mo, P, and S was confirmed by EDX (Kα, Lα). FAB-DP$^+$-MS (nitrobenzyl alcohol as matrix, CH_2Cl_2): $m/z = 957$ ($(M + 3H)^+$, relative intensity 34%), 561 ($(M -$ dppee$)^+$, 22). There were also peaks found at $m/z = 939$ (31%) and 545 (25%). These signals correspond to the oxidized complex of the composition Mo(O)(S)(dppee)$_2$ (M + 3H and M − dppee). The oxidation of the complexes $Mo(Q)_2$(dppee)$_2$ (Q = S, Se, Te) by the matrix used in the FAB-MS experiment became more predominant in the case of the heavier chalcogens (Se, Te). The calculated isotopic pattern at $m/z = 957$ is in good agreement with the recorded values. UV/vis (CH_2Cl_2, nm (relative intensity of the bands)): 547 (0.5), 433 (6, sh), 414 (10, sh), 374 (100), 319 (51).

Preparation of *trans*-Mo(Se)$_2$(dppee)$_2$ (3). A 250 mg sample of *trans*-$Mo(N_2)_2$(dppee)$_2$ (0.26 mmol), 75 mg of elemental selenium (0.95 mmol), and 5 mg of dppee were suspended in 20 mL of toluene, and the suspension was heated overnight to 90−100 °C. The suspension turned from dirty orange to dark brown, and a very dark precipitate formed. The light orange mother liquor was filtered off and discarded. The residue was washed several times with 20 mL portions of toluene and diethyl ether. Finally the residue was extracted with dichloromethane, and the extract was layered with hexane. After 1 week, well-formed green crystals of ***trans*-Mo(Se)$_2$(dppee)$_2$·CH$_2$Cl$_2$** were collected (60 mg, 20%). The extraction with CH_2Cl_2 should be repeated several times to increase the yield. A small amount of brown precipitate (60 mg) was also formed but not further characterized.

***trans*-Mo(Se)$_2$(dppee)$_2$ (3):** mp = 250−251 °C dec; $^{31}P\{^1H\}$ NMR (81 MHz, CH_2Cl_2, room temperature) $\delta = 50.4$ ppm (singlet). The presence of the heavier elements Mo, P, Se, and Cl (solvent in the lattice) was confirmed by EDX (Kα, Lα). No mass spectrum could be obtained. UV/vis (CH_2Cl_2, nm (relative intensity of the bands)): 637 (0.2), 585 (0.3), 520 (3), 414 (100), 322 (35).

Preparation of *trans*-Mo(Te)$_2$(dppee)$_2$ (4). A solution of $TePEt_3$ was prepared by stirring 250 mg of elemental tellurium (2.0 mmol) and 0.15 mL of PEt_3 in 10 mL of toluene for 1 h. This suspension was added to a solution of 270 mg of *trans*-$Mo(N_2)_2$(dppee)$_2$ (0.29 mmol) in 20 mL of toluene. The reaction mixture was heated to 90 °C for 2 h, and another portion of the $TePEt_3$/Te/PEt_3 suspension was added. Overnight, the suspension became dark green. The only slightly green mother liquor was filtered off and discarded. The residue was washed with 20 mL portions of diethyl ether, once with toluene, and twice with hexane. ***trans*-Mo(Te)$_2$(dppee)$_2$** was extracted repeatedly with CH_2Cl_2 (yield 125 mg, 38%). One of the CH_2Cl_2 extracts was layered with 5 mL of THF and subsequently with hexanes, yielding very small green crystals of ***trans*-Mo(Te)$_2$(dppee)$_2$**.

***trans*-Mo(Te)$_2$(dppee)$_2$ (4):** $^{31}P\{^1H\}$ NMR (81 MHz, CH_2Cl_2, room temperature) $\delta = 48.7$ ppm (singlet). The presence of the heavier elements Mo, P, and Te was confirmed by EDX (Kα, Lα). No FAB mass spectrum (matrix nitrobenzyl alcohol, solvent CH_2Cl_2) could be obtained. UV/vis (CH_2Cl_2, nm (relative intensity of the bands)): 807 (0.2, sh), 773 (0.4), 624 (22), 485 (100), 386 (20, sh), 352 (29, sh), 320 (39, sh).

Preparation of *trans*-Mo(S)$_2$(dppe)$_2$ (5). A 237 mg sample of *trans*-$Mo(N_2)_2$(dppe)$_2$ (0.25 mmol) and 140 mg of dibenzyl trisulfide (0.5 mmol) were dissolved in 40 mL of toluene. Upon being heated to 30 °C, the reaction mixture became dark brown. After the mixture was cooled to room temperature, a small amount of precipitate was filtered off and the solution was layered with hexanes. After 2 weeks, thin green plates of ***trans*-Mo(S)$_2$(dppe)$_2$·$^1/_2$tol** (tol = toluene) were manually picked out of the tube (yield 60 mg, 24%). Some brown precipitate was also formed but not further characterized. The synthesis also worked in other solvents, e.g. THF and benzene. **5**·$^1/_2$THF and **5**·$^1/_2C_6H_6$ are isostructural with **5**·$^1/_2$tol.

***trans*-Mo(S)$_2$(dppe)$_2$ (5):** mp 214 °C dec; $^{31}P\{^1H\}$ NMR (81 MHz, CH_2Cl_2, room temperature) $\delta = 37.4$ ppm (singlet). The presence of the heavier elements Mo, P, and S was confirmed by EDX (Kα, Lα). FAB-DP$^+$-MS (nitrobenzyl alcohol as matrix, CH_2Cl_2): $m/z = 961$ ($(M + 3H)^+$, relative intensity 63%), 563 ($(M -$ dppee$)^+$, 48). There were also peaks found at $m/z = 945$ (16%) and 546 (16%). These signals correspond to the oxidized complex of the composition Mo(O)(S)(dppe)$_2$ (M + 3H and M − dppee). The calculated isotopic pattern at $m/z = 961$ is in good agreement with the recorded values. When 2-nitrophenyl octyl ether was used as the FAB matrix, signals of the unprotonated parent ions could be obtained in a very noisy spectrum ($m/z = 958$ (M^+), 557 ($(M -$ dppee$)^+$). In this case the oxidation of the complex was suppressed. UV/vis (CH_2Cl_2, nm (relative intensity of the bands)): 547 (0.6), 431 (8, sh), 380 (100), 340 (57), 320 (51, sh).

(4) Dilworth, J. R.; Richards, R. L.; Chen, G. J.-J.; McDonald, J. W. *Inorg. Synth*. **1980**, *20*, 119.
(5) Anker, M. W.; Chatt, J.; Leigh, G. J.; Wedd, A. G. *J. Chem. Soc., Dalton Trans*. **1975**, *23*, 2639.
(6) Cotton, F. A.; Schmid, G. Unpublished results.

Table 1. Crystal and Structure Refinement Data

	1	**2**	**3**	**4**	**5**	**6**	**7**	**8**
empirical formula	$C_{52}H_{44}MoO_2P_4$	$C_{52}H_{44}MoP_4S_2$	$C_{52}H_{44}MoP_4Se_2$	$C_{52}H_{44}MoP_4Te_2$	$C_{52}H_{48}MoP_4S_2$	$C_{52}H_{48}MoP_4Se_2$	$C_{52}H_{44}MoOP_4S$	$C_{52}H_{44}MoO_4P_4S_2$
lattice solvent/ formula unit	$2CH_4O$		CH_2Cl_2		$^1/_2C_7H_8$	$^1/_2C_7H_8$		
fw	984.84	952.81	1131.54	1143.89	1002.91	1096.71	936.75	1016.81
space group	$P2_1/c$ (No. 14)	$P\bar{1}$ (No. 2)	$P2_1/c$ (No. 14)	$P\bar{1}$ (No. 2)	$C2/c$ (No. 15)	$C2/c$ (No. 15)	$P\bar{1}$ (No. 2)	$C2/c$ (No.15)
crystal system	monoclinic	triclinic	monoclinic	triclinic	monoclinic	monoclinic	triclinic	monoclinic
unit cell dimens								
a, Å	11.1340(15)	10.102(4)	11.186(5)	12.681(4)	49.515(7)	49.566(9)	10.040(1)	21.534(6)
b, Å	18.435(2)	10.722(4)	18.005(8)	19.280(5)	10.9286(12)	10.9765(15)	10.563(1)	12.4271(13)
c, Å	12.515(2)	12.195(3)	12.761(9)	10.454(3)	18.203(3)	18.282(3)	12.162(2)	19.550(5)
α, deg		100.95(3)		104.60(2)			75.30(1)	
β, deg	110.999(9)	95.04(4)	110.35(4)	111.61(2)	98.306(12)	98.541(13)	85.93(1)	118.480(14)
γ, deg		117.81(2)		75.12(2)			63.21(1)	
V, Å^3	2398.3(5)	1123.1(7)	2410(2)	2261.1(11)	9747(3)	9836(3)	1112.3(2)	4598(2)
Z	2	1	2	2	8	8	1	4
d_{calc}, g/cm^3	1.364	1.409	1.560	1.680	1.367	1.481	1.398	1.469
crystal size, mm^3	0.5 × 0.3 × 0.2	0.5 × 0.5 × 0.15	0.3 × 0.2 × 0.15	0.2 × 0.05 × 0.05	0.5 × 0.4 × 0.08	0.5 × 0.5 × 0.06	0.4 × 0.2 × 0.1	0.5 × 0.3 × 0.2
μ, mm^{-1}	0.452	0.564	2.063	13.960	0.523	1.914	4.504	0.562
λ, Å	0.710 73	0.710 73	0.710 73	1.541 84	0.710 73	0.710 73	1.541 84	0.710 73
no. of orient. reflns; θ range, deg	200; 13−18	200; 13−18	1000; 8−21	65; 5−23	200; 13−18	200; 13−16	25; 29−38	197; 14−18
temp, K	293(2)	293(2)	213(2)	293(2)	293(2)	293(2)	293(2)	293(2)
scan method	$\omega/2\theta$	ω scan	ω rot., 0.2°, 40 s	$\omega/2\theta$	$\omega/2\theta$	ω/θ	$\omega/2\theta$	$\omega/(1/3)\theta$
θ range for data colln, deg	2.1−24.0	2.2−25.4	2.3−24.0	2.4−60.0	2.2−23.9	2.2−22.9	3.8−60.1	2.0−24.9
no. of reflns collected	3949	5205	11 257	7090	8276	7073	3313	5064
no. of unique reflns, R_{int}	3759, 0.017	4166, 0.021	3579, 0.098	6736, 0.048	7600, 0.031	6811, 0.028	3313, 0.0	4036, 0.021
no. of data, restraints, params	3758, 0, 296	4166, 0, 340	3442, 0, 282	6735, 0, 539	6507, 0, 589	6811, 0, 551	3313, 0, 281	4035, 0, 293
transm range	0.97−1.00	0.75−1.00		0.71−1.00	0.87−1.00	0.69−1.00	0.57−1.00	0.91−1.00
final R_1, R_2 [$I > 2\sigma(I)$]	0.032, 0.080	0.037, 0.097	0.065, 0.140	0.050, 0.117	0.040, 0.095	0.061, 0.174	0.030, 0.098	0.030, 0.075
final R_1, R_2 (all data)	0.049, 0.087	0.046, 0.103	0.100, 0.168	0.119, 0.142	0.089, 0.111	0.097, 0.197	0.030, 0.098	0.044, 0.081
goodness-of-fit on F^2	1.046	1.077	1.079	1.047	1.038	1.064	1.102	1.031
largest peak, e/Å^3	0.69(6)	0.98(8)	1.47(16)	0.91(16)	0.51(6)	0.91(15)	0.33(6)	0.66(6)

Preparation of *trans*-Mo(Se)$_2$(dppe)$_2$ (6). A 238 mg sample of *trans*-Mo(N$_2$)$_2$(dppe)$_2$ (0.25 mmol), 63 mg of elemental selenium (0.8 mmol), and 2 mg of dppe were heated to 90−95 °C in 30 mL of toluene for 4 h. The reaction mixture became greenish brown. After the mixture was cooled to room temperature, excess Se was filtered off and the filtrate layered with hexane. After 1 day, large, brown, thin plate-shaped crystals of ***trans*-Mo(Se)$_2$(dppe)$_2$·$^1/_2$tol** appeared on the walls of the Schlenk tube and were collected (yield 135 mg, 49%).

***trans*-Mo(Se)$_2$(dppe)$_2$ (6):** mp 197−199 °C dec; ^{31}P{^{1}H} NMR (81 MHz, CH_2Cl_2, room temperature) $\delta = 36.5$ ppm (singlet). The presence of the heavier elements Mo, P, and Se was confirmed by EDX (Kα, Lα). The matrix nitrobenzyl alcohol used for FAB mass spectrometry oxidized **6**, but Se-containing fragments could be seen. FAB-DP$^+$-MS (nitrobenzyl alcohol as matrix, CH_2Cl_2): $m/z = 1009$ ((M − Se + 2O + 2H)$^+$, relative intensity 6%), 611 ((M − Se + 2O + 2H − dppee)$^+$, 4%). The calculated isotopic pattern at $m/z = 1009$ is in good agreement with the recorded values. UV/vis (CH_2Cl_2, nm (relative intensity of the bands)): 598 (0.3), 514 (4), 420 (100), 343 (52, sh), 320 (59, sh).

Preparation of *trans*-Mo(O)(S)(dppee)$_2$ (7). **7** was obtained by the reaction of $MoCl_3(THF)_3$, dppee, and an excess of NaHS in a mixture of THF and methanol. The structure was unequivocally established by X-ray crystallography. However, the reaction itself could not be repeated well. In an attempt to prepare **7** by a rational synthesis, **8** (see below) was obtained.

Preparation of *trans*-Mo(SO$_2$)$_2$(dppee)$_2$ (8). Gaseous sulfur dioxide was bubbled through a solution of 195 mg of *trans*-Mo(N$_2$)$_2$(dppee)$_2$ (0.21 mmol) in 50 mL of toluene for 30 min. The initial orange solution became dark green, and subsequently a yellow precipitate formed, which was filtered off and washed twice with 5 mL of diethyl ether. After the solid was dissolved in 15 mL of CH_2Cl_2 and the solution was layered with 5 mL of THF, followed by 40 mL of hexanes, nice yellow crystals appeared over a period of 2 weeks (yield 85 mg, 40%).

Mo(SO$_2$)$_2$(dppee)$_2$ (8). No signals were observed in the ^{31}P{^{1}H} NMR because of the paramagnetism of the compound. The presence of the heavier elements Mo, P, and S was confirmed by EDX (Kα, Lα). FAB-DP$^+$-MS (nitrobenzyl alcohol as matrix, CH_2Cl_2): no parent ion was found; $m/z = 970$ ((M − SO)$^+$, relative intensity 37%), 953 ((M − SO$_2$)$^+$, 21), 941 ((M − SO$_3$)$^+$, 100), 921/923 ((Mo(O)$_2$(dppee)$_2$$^+$/ Mo(S)(dppee)$_2$$^+$, 53)). The calculated isotopic patterns are in good agreement with those measured. The composition of the fragments was confirmed by accurate mass determinations. UV/vis (CH_2Cl_2, nm): 304. IR (KBr, cm^{-1}): $\nu_{S-O} = 1092$.

X-ray Crystallography. Crystals of the compounds **1**−**8** were mounted onto glass fiber tips. Epoxy glue was used for measurements at room temperature (293(2) K) and silicone grease for measurements at 213(2) K. In all cases, the crystals were stable during measurement (<5% decay). Lorentz and polarization corrections but no time-dependent corrections were applied to the raw data. The Laue groups were confirmed by axial photographs.

Diffraction intensities for **1**, **2**, **5**, **6**, and **8** were collected on an Enraf-Nonius CAD4 diffractometer using Mo Kα radiation ($\lambda = 0.710\ 73$ Å). The ratio of the movements of the ω and θ angles was determined from two-dimensional reflection profile plots (Table 1). Empirical absorption corrections (ψ scans) were applied to the data sets of **1**, **2**, and **8**. Compounds **5** and **6** crystallized in the shape of very thin plates. To minimize the absorption correction, the data were collected in such a manner that the sum of the path lengths of the incident and diffracted beams was minimized as a function of the azimuthal angle ψ using the model of an imaginary crystal with finite but small thickness having an infinite surface area (Mode FLAT). Accurate unit cell dimensions

were determined by a least-squares fit to the θ angles of about 200 accurately centered reflections.[7]

Diffraction intensities for **3** were collected on an Enraf-Nonius FAST area detector system (sealed tube, Mo anode, $\lambda = 0.710\ 73$ Å) equipped with a low-temperature unit. The unit cell dimensions were determined by a least-squares fit to 1000 centered reflections at a detector swing angle of 0° (ω between 0 and 150°, θ between 8 and 21°). Subsequently, images were collected at four different goniometer positions by ω oscillation (0.2° steps, 40 s per image). Reflection intensities were evaluated by the best-fit ellipsoid method.[8]

Diffraction intensities for **4** and **7** were collected on an MSC Rigaku AFC5R diffractometer equipped with a rotating Cu anode ($\lambda = 1.541\ 84$ Å). Empirical absorption corrections (ψ scans) were applied[9] in both cases. Only very small highly twinned needle-shaped crystals of **4** could be obtained. After examination of about 10 crystals, one was selected where the twin components could be separated manually with the help of DIRAX.[10]

All structures were solved by the tangent formula or Patterson method provided by SHELXS-86[11] and refined with full-matrix least-squares calculations based on F^2 applying a variance-based weighting scheme (SHELXL-93[12]). All non-hydrogen atoms were refined with anisotropic temperature factors (exception: the disordered, half-occupied O atom in **7**). Hydrogen atoms were usually included in the refinement at calculated positions riding on the pivotal C atoms. For **1**, **5**, **7**, and **8**, hydrogen atoms bonded to ethylene and ethane bridges were allowed to refine. For **2**, all hydrogen atoms were found in the Fourier map and were refined with a common temperature factor.

Solvents in the Lattices. **1** crystallized with two methanol molecules per formula unit, related by an inversion center. The methyl group of the solvent molecule was found to be equally disordered over two positions. The hydrogen atom of the hydroxyl group was neglected in the refinement. **3** crystallized with a dichloromethane solvent molecule which was equally disordered over two positions around an inversion center. All solvent hydrogen atoms were omitted in the refinement. In **5** and **6**, a toluene molecule was disordered over several positions around a 2-fold axis. No reasonable connectivities could be found. Some of the highest peaks were used to model the solvent molecule. In the case of **5**, the reaction was also conducted in benzene and THF. **5**·$^1/_2C_6H_6$ (monoclinic; $a = 49.242(8)$ Å, $b = 10.8961(12)$ Å, $c = 18.180(3)$ Å, $\beta = 97.509(12)$°; room temperature) and **5**·$^1/_2$-THF (monoclinic; $a = 49.263(8)$ Å, $b = 10.910(7)$ Å, $c = 18.047(2)$ Å; $\beta = 98.84(3)$°; −100 °C) are isostructural with **5**·$^1/_2$tol. These compounds crystallized also as very thin plates. In the data set of **5**·$^1/_2$THF, the THF solvent molecule could be located around the 2-fold axis. However, the data set was measured on the FAST area detector system (analogous to the procedure for **3**). The method already discussed for minimizing absorption in **5** and **6** proved to yield much better data sets.

The ORTEP program was used to draw the representations of **1**−**8**.[7] Crystal and refinement data for **1**−**8** are summarized in Table 1. The atomic positional parameters have been deposited with the Cambridge Crystallographic Data Center.

Results and Discussion

Only a few compounds of the type *trans*-Mo(Q)(Q′)(P⌒P)$_2$, where Q and Q′ are chalcogen ligands (O, S, Se, Te), are known in the literature. Quite often, the compounds were obtained unintentionally or as decomposition products due to the presence of air and moisture. In some cases, it was difficult to decide whether the complexes were neutral or cationic, particularly in the case of protonated *trans*-[Mo(QH)(Q′)(P⌒P)$_2$]$^+$ species. Therefore one of our goals was to develop rational synthetic routes. The discussion is extended to compounds with other ligands in the equatorial positions, especially sulfur or CN^-.

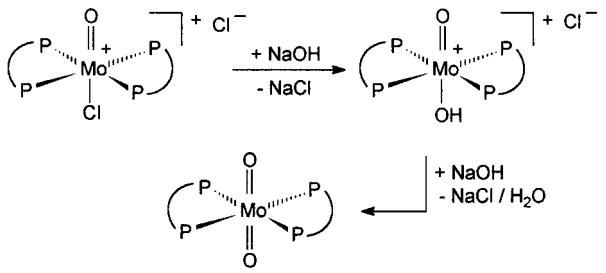

Figure 2. Preparation of *trans*-Mo(O)$_2$(dppee)$_2$ (**1**) by hydrolyis of [*trans*-Mo(O)(Cl)(dppee)$_2$]Cl and subsequent deprotonation (P⌒P = dppee).

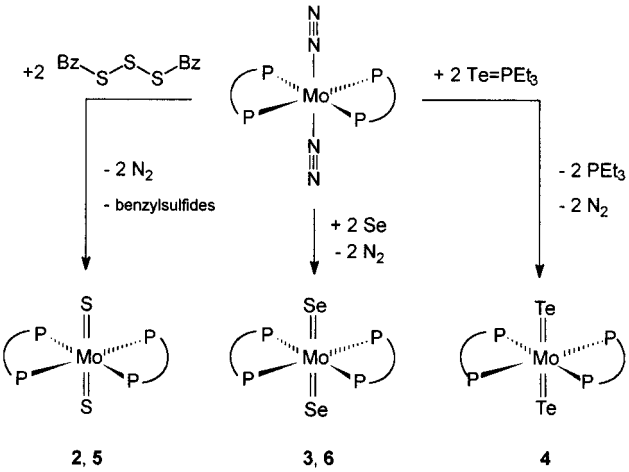

Figure 3. Preparation of complexes of the type *trans*-Mo(Q)$_2$ (P⌒P)$_2$, **2** (Q = S), **3** (Q = Se), and **4** (Q = Te) (P⌒P = dppee) and **5** (Q = S) and **6** (Q = Se) (P⌒P = dppe), by the reaction of *trans*-Mo(N$_2$)$_2$(P⌒P)$_2$ and a chalcogen source.

Synthesis. *trans*-Mo(O)$_2$(dppee)$_2$ (**1**) is the first complex of the type in question where two nonprotonated oxygen atoms occupy the axial positions. It was obtained by a hydrolysis reaction of *trans*-[Mo(O)(Cl)(dppee)$_2$]Cl (Figure 2). First, we obtained **1** as nice, slightly yellow crystals by the evaporation of a solution of *trans*-[Mo(O)(Cl)(dppee)$_2$]Cl in methanol containing the highly hygroscopic base HS^- and S^{2-} and in the presence of air and moisture. The driving force for the deprotonation step is the volatility of H_2S. Later, a more direct route for the preparation of this compound was developed: the reaction between *trans*-[Mo(O)(Cl)(dppee)$_2$]Cl and NaOH in methanol. In this reaction, special care must be taken to ensure the completeness of the deprotonation step, by raising the pH to 8.

Churchill et al. described the X-ray structure of an example of the proposed protonated intermediate *trans*-[Mo(O)(OH)-(dppe)$_2$]$^+$[BF$_4$]$^-$.[13] While the source of this product was not clear, it was suggested that it resulted from the reaction between HMo(dppe)$_2^+$ and adventitious O_2.

A parent ion signal $(M + H)^+$ of **1** was observed by FAB mass spectrometry when nitrobenzyl alcohol was used as matrix.

Compounds **2**−**6** were obtained by the reaction between the Mo(0) complexes *trans*-Mo(N$_2$)$_2$(P⌒P)$_2$ and a chalcogen source (Figure 3). Despite the high similarity between dppee and dppe, **2** and **3** are much less soluble than **5** and **6** in solvents like THF, toluene, and CH_2Cl_2.

(7) Brüggemann, R.; Debaerdemaeker, T.; Müller, B.; Schmid, G.; Thewalt, U. Ulm-Programmsystem. Preprint of Suppl. 5, *Z. Kristallogr.*, 33.
(8) Kabsch, W. *J. Appl. Crystallogr.* **1988**, *21*, 916.
(9) TEXSAN-TEXRAY: *Structure Analysis Package*; Molecular Structure Corp.: The Woodlands, TX, 1985.
(10) Duisenberg, A. J. M. *J. Appl. Crystallogr.* **1992**, *25*, 92.
(11) SHELXS-86: Sheldrick, G. M. *Acta Crystallogr.* **1990**, *A46*, 467.
(12) SHELXL-93: Sheldrick, G. M. Program for structure refinement. University of Göttingen, 1993. Sheldrick, G. M. *J. Appl. Crystallogr.* **1993**, in preparation.
(13) Churchill, M. R.; Rotella, F. J. *Inorg. Chem.* **1978**, *17*, 668.

The oxidation of *trans*-$Mo(N_2)_2(dppee)_2$ and *trans*-$Mo(N_2)_2(dppe)_2$ with dibenzyl trisulfide in toluene gave brown *trans*-$Mo(S)_2(dppee)_2$ (**2**) and green *trans*-$Mo(S)_2(dppe)_2$ (**5**), respectively. Simultaneously with our work, Murphy and Parkin showed that the more reactive and less sterically demanding systems $Mo(PMe_3)_6$ (Me = methyl) and $Mo(PMe_3)_4(\eta^2\text{-}CH_2PMe_2)H$ can react with H_2S to yield *trans*-$Mo(S)_2(PMe_3)_4$.[14] In the literature *t*-BuSH (Bu = butyl) or S_8 was shown to introduce the chalcogen in the reaction with $Mo(N_2)_2$(*syn*-Me_8[16]aneS_4).[15] However, in our hands, the reaction with elemental sulfur yielded only intractable, insoluble brown materials presumably due to the cleavage of the Mo−P bond and formation of species of higher nuclearity or MoS_2.

The identity of **2** and **5** was confirmed by FAB mass spectrometry and X-ray crystallography (see below). When nitrobenzyl alcohol was used as a matrix, protonated parent ion signals could be seen: $(M + 3H)^+$. However, this matrix also oxidizes **2** and **5**, and signals of species of the composition $(Mo(O)(S)(\overset{\frown}{P}P)_2 + 3H)^+$ were observed. The protonation and oxidation could be completely suppressed by using 2-nitrophenyl octyl ether as the FAB matrix, but then only a very noisy spectrum was obtained from **5**. No FAB spectra in 2-nitrophenyl octyl ether were obtained for **2** due to the very low solubility. The oxidation of the complexes $Mo(Q)(Q')(\overset{\frown}{P}P)_2$ became predominant for compounds of the heavier chalcogens (Se, Te).

trans-$Mo(Se)_2(dppee)_2$ (**3**) and *trans*-$Mo(Se)_2(dppe)_2$ (**6**) were prepared by oxidation of the N_2 precursors with elemental selenium. Catalytic amounts of dppee and dppe were added to promote the breakup of the Se powder by the formation of phosphine selenides as carrier reagents. The mass spectrum of **3** could not be obtained. In the FAB mass spectrum (nitrobenzyl alcohol as matrix) of **6**, only signals of oxidized species were observed [m/z = 1009 ($(M - Se + 2O + 2H)^+$) and 611 ($(M - Se + 2O + 2H - dppee)^+$)].

trans-$Mo(Te)_2(dppee)_2$ (**4**) could not be prepared by reacting elemental tellurium with *trans*-$Mo(N_2)_2(dppee)_2$. It was necessary to add a large excess of PEt_3 (Et = ethyl) for the formation of $TePEt_3$ as carrier reagent. No FAB mass spectrum of **4** could be obtained.

trans-$Mo(O)(S)(dppee)_2$ (**7**) was first obtained by reacting $MoCl_3(THF)_3$ with an excess of NaHS and dppee in a mixture of methanol and THF. Because the role of moisture and air in this reaction was not clear, an alternative route was devised. Lorenz et al. reported the preparation of *trans*-$Mo(O)(S)(dppe)_2$ from the reaction between *trans*-$Mo(N_2)_2(dppe)_2$ and sulfur dioxide.[16] The reaction mechanism was not clear in this case either, but formally two SO_2 molecules disproportionate into SO_3 and SO. The latter is then oxidatively added to the $Mo(dppee)_2$ moiety. Some evidence for the proposed mechanism was found in the crystal structure because SO_2 and H_2SO_4 were observed in the lattice. Though the authors of ref 16 claimed that they were not able to repeat the reaction,[17] we were able to repeat the reaction and confirmed their results. The $^{31}P\{^1H\}$ NMR (δ = 40.1 ppm; reported 39.2 ppm) and IR data (ν(MoO) = 946 cm^{-1} (m), ν(MoS) = 480 cm^{-1} (w)), melting point (191 °C dec; reported 185 °C), mass spectrometry (M + 3H), and blue-violet color of *trans*-$Mo(O)(S)(dppe)_2$ are all in good agreement with the reported observations. The same reaction yielded $Mo(SO_2)_2(dppee)_2$ (**8**) if dppee instead of dppe was used as the bidentate phosphine ligand (Figure 4).

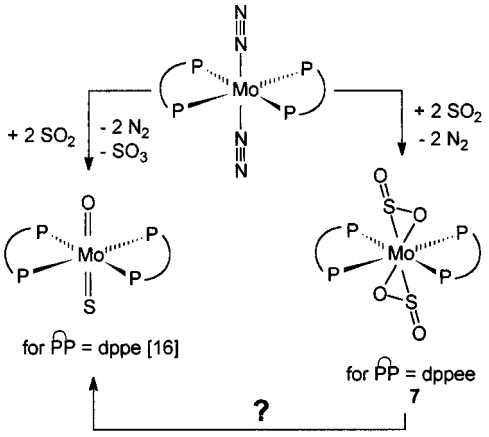

Figure 4. Reaction of *trans*-$Mo(N_2)_2(\overset{\frown}{P}P)_2$ type complexes with SO_2. The products depend upon the use of dppe or dppee as equatorial ligands.

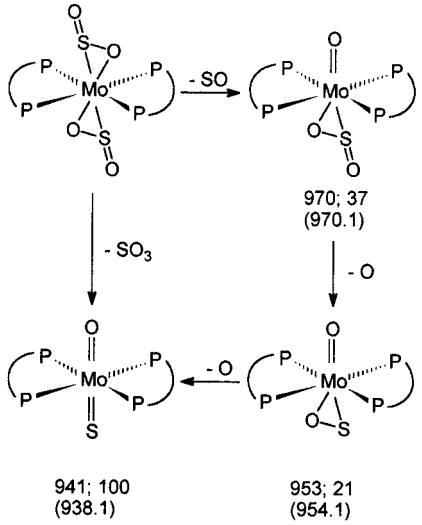

Figure 5. Proposed intermediates on the pathway from $Mo(SO_2)_2(\overset{\frown}{P}P)_2$ type complexes to $Mo(O)(S)(\overset{\frown}{P}P)_2$ type complexes ($\overset{\frown}{P}P$ = dppee). The numbers below the structures indicate the masses of the ions found by FAB mass spectrometry; the numbers in brackets indicate the calculated values. The addition of hydrogen atoms was neglected.

Table 2. ^{31}P NMR Shifts for Compounds of the Type $Mo(Q)(Q')(P)_4$

	(O)(O)	(S)(S)	(Se)(Se)	(Te)(Te)	(O)(S)	ref
PMe_3		−14.0	−16.0	−16.2		14
dppe		37.4	36.5		39.2; 40.1	16; this work
dppee	49.3	50.5	50.4	48.7		this work

No formation of **7** was observed. FAB mass spectrometry (matrix nitrobenzyl alcohol) provided some information regarding the composition of possible intermediates along the pathway from $Mo(SO_2)_2(\overset{\frown}{P}P)_2$ type complexes to *trans*-$Mo(O)(S)(\overset{\frown}{P}P)_2$ type complexes. The proposed structures of the intermediates are summarized in Figure 5.

$^{31}P\{^1H\}$ Spectroscopy. The ^{31}P shifts of known complexes of the type $Mo(Q)(Q')(P)_4$ are summarized in Table 2. In all cases, a singlet is observed. The chemical shifts are constant within 2 ppm for a given phosphine ligand and Q = Q′. Only a slightly larger difference is found when Q = O, Q′ = S, and dppe is the diphosphine. For a given series of Q, the ^{31}P shifts vary according to the basicity of the axial ligand, with more basic ligands shifting the ^{31}P signal to higher field. It seems that the orbital set used for the formation of the equatorial bonds ($d_{x^2-y^2}$, d_{xy}) is virtually independent (orthogonal) of the set used for the formation of the axial bonds (d_{z^2}, d_{xz}, d_{yz}). The d_{xz} and d_{yz} orbitals contribute almost exclusively to the π interac-

(14) Murphy, V. J.; Parkin, G. *J. Am. Chem. Soc.* **1995**, *117*, 3522.
(15) Yoshida, T.; Adachi, T.; Matsumura, K.; Kawazu, K.; Baba, K. *Chem. Lett.* **1991**, 1067.
(16) Lorenz, I.-P.; Walter, G.; Hiller, W. *Chem. Ber.* **1990**, *123*, 979.
(17) Lorenz, I.-P. Private communication.

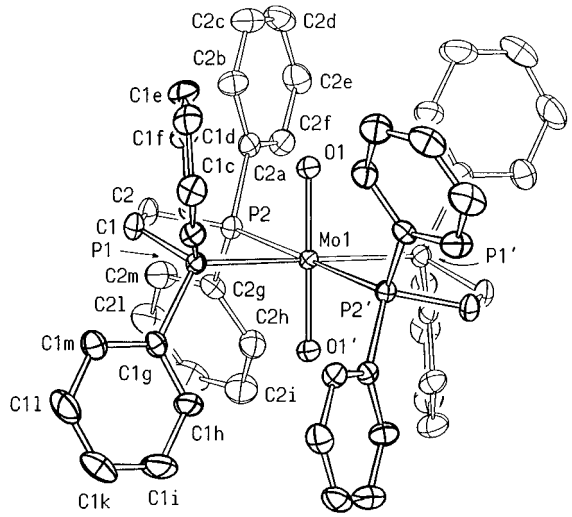

Figure 6. Molecular structure representation and atom-numbering scheme of *trans*-$Mo(O)_2(dppee)_2$ (**1**).

Table 3. Selected Bond Lengths (Å) and Angles (deg) for *trans*-$Mo(O)_2(dppee)_2$ (**1**)·$2CH_3OH$[a]

Mo(1)−O(1)	1.804(2)		
Mo(1)−P(1)	2.5095(7)	Mo(1)−P(2)	2.5040(8)
P(1)−C(1)	1.826(3)	P(2)−C(2)	1.825(3)
P(1)−C(1a)	1.820(3)	P(2)−C(2a)	1.823(3)
P(1)−C(1g)	1.820(3)	P(2)−C(2g)	1.827(3)
C(1)−C(2)	1.309(4)		
O(1)−Mo(1)−P(1)	85.18(6)	O(1)−Mo(1)−P(2)	85.39(7)
O(1)−Mo(1)−P(1)^i	94.82(6)	O(1)−Mo(1)−P(2)^i	94.61(7)
P(2)−Mo(1)−P(1)	80.11(2)	P(2)−Mo(1)−P(1)^i	99.89(2)
C(1)−P(1)−C(1a)	101.66(14)	C(2)−P(2)−C(2a)	101.77(14)
C(1)−P(1)−C(1g)	102.64(14)	C(2)−P(2)−C(2g)	102.39(14)
C(1a)−P(1)−C(1g)	103.56(13)	C(2a)−P(2)−C(2g)	103.14(13)
P(1)−C(1)−C(2)	121.8(2)	P(2)−C(2)−C(1)	121.5(2)

[a] Symmetry transformation used to generate equivalent atoms: (i) $-x, -y, -z$.

tions with the axial chalcogen ligands and have negligible contributions to π back-bonding to the phosphorus atoms.

X-ray Crystallography. The molecular structure of complexes **1**−**7** is close to a distorted octahedron with an equator defined by the phosphorus atoms and the chalcogen atoms at the apices. The point group symmetry of **1**−**6** is close to D_{2h}. The two different chalcogen atoms in the apical positions in **7** lower the symmetry to C_{2v}. The inversion center of the point group D_{2h} is crystallographically realized when P⌒P is dppee. The molecules of **1**−**4** and **7** (pseudo inversion center due to disorder) reside on inversion centers; the molecular structure possesses full C_i symmetry.

trans-$Mo(O)_2(dppee)_2$ (**1**) is the first example of a neutral complex with a *trans*-$Mo(O)_2$ moiety (Figure 6). **1** crystallizes in the monoclinic space group $P2_1/c$ with methanol solvent molecules hydrogen-bridged to the axial oxygen atoms (O(1)···O(3) = 2.710(4) Å, Mo−O(1)···O(3) = 170.88(14)°). Selected bond distances and angles are summarized in Table 3.

In **1** the Mo(1)−O(1) bond distance was found to be 1.804(2) Å. Robinson et al. have compiled a table of Mo(IV)═O bond lengths, which range from 1.668(5) Å in Mo(O)$(H_2O)(CN)_4^{2-}$ to 1.834(9) Å in *trans*-$Mo(O)_2(CN)_4^{4-}$.[18,19] Since the Mo═O bond length in $Mo(O)(H_2O)(CN)_4^{2-}$ is significantly shorter than that in **1,** a significant triple-bond contribution has to be assumed. Both the d_{xz} and d_{yz} orbitals on the Mo atom interact with the p_x and p_y orbitals on *one* O atom because there is no possibility for a π interaction at the O atom on the coordinated water molecule. Therefore a bond length of approximately 1.67 Å should be regarded as the lower limit for these Mo═O "double" bonds. When there are two coordinated O atoms in the axial positions, their p_x and p_y orbitals mix to yield one set with e_{1u} and another one with e_{1g} symmetry. Only the set with e_{1g} symmetry is able to interact with the d_{xz}(Mo) and d_{yz}(Mo) orbitals. In this case, only a "pure" double bond between Mo and O is possible. The bond lengths in **1** and *trans*-$Mo(O)_2(CN)_4^{4-}$ [19] are equal within 3σ. This fact again demonstrates that the d_{xz} and d_{yz} orbitals are primarily involved in metal−ligand multiple bonding with the axial ligands as was already seen in the $^{31}P\{^1H\}$ NMR spectra. The slightly greater bond lengths in *trans*-$Mo(O)_2(CN)_4^{4-}$ in comparison to those in **1** may be attributed to the high charge on the complex. If the π contribution to the bonding is lost, for example by protonating one O atom, the Mo−OH bond length falls into the range from 1.952(5) Å for [*trans*-$Mo(O)(OH)(dppe)_2]^+$ [13] to 2.077(7) Å for $Mo(O)(OH)(CN)_4^{3-}$.[18] In the latter, O/OH disorder problems were reported. We also obtained crystals where **1** and $[Mo(O)(OH)(dppee)_2]Cl$ are cocrystallized in an approximately 1:1 ratio if the deprotonation of Mo(O)(OH)-$(dppee)_2^+$ is not complete. A satisfactory refinement of this structure was not possible.[20]

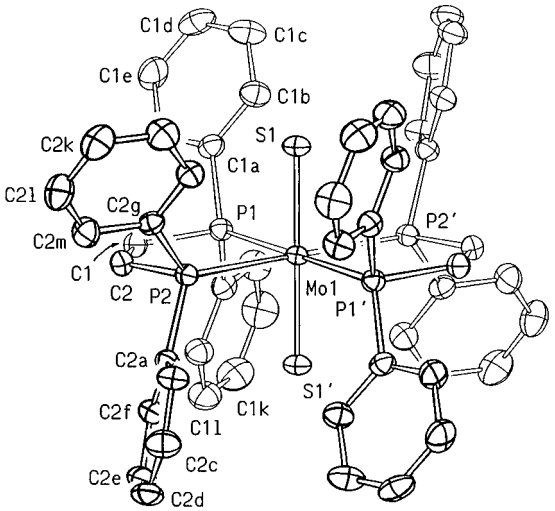

Figure 7. Molecular structure representation and atom-numbering scheme of *trans*-$Mo(S)_2(dppee)_2$ (**2**).

Two examples of the *trans*-$Mo(S)_2(P⌒P)_2$ type complex have been prepared. *trans*-$Mo(S)_2(dppee)_2$ (**2**) crystallized in the space group $P\bar{1}$ residing on a crystallographic inversion center (Figure 7). *trans*-$Mo(S)_2(dppe)_2$ (**5**) was found on a general position in the space group $C2/c$ (Figure 8). The positional and isotropic equivalent temperature parameters of **2** and **5** are listed in the Tables 5 and 7. The selected bond distances and angles of **2** and **5** are compiled in Tables 4 and 5, respectively. It should be noted that the views in Figures 7 and 8 are different. Figure 7 is viewed in a direction perpendicular to the chelating P⌒P ligand while Figure 8 is viewed toward it.

The Mo═S bond distances are almost equal in **2** (2.228(1) Å) and **5** (Mo(1)═S(1) = 2.236(1) Å and Mo(1)═S(2) = 2.249(1) Å), the S═Mo═S bond angles being 180 and 175.51(4)°, respectively. As mentioned before, the basicity of the phosphine ligand in the equatorial position has only a minor influence on the bond lengths and bond angles. In *trans*-$Mo(S)_2(PMe_3)_4$,

(18) Robinson, P. R.; Schlemper, E. O.; Murmann, R. K. *Inorg. Chem.* **1975**, *14*, 2035.
(19) Day, V. W.; Hoard, J. L. *J. Am. Chem. Soc.* **1968**, *90*, 3374.

(20) Monoclinic, space group $P2_1/a$ (presumably); a = 12.3523(6) Å, b = 18.3003(6) Å, c = 21.8948(9) Å, β = 92.494(2)°; temperature −75 °C.

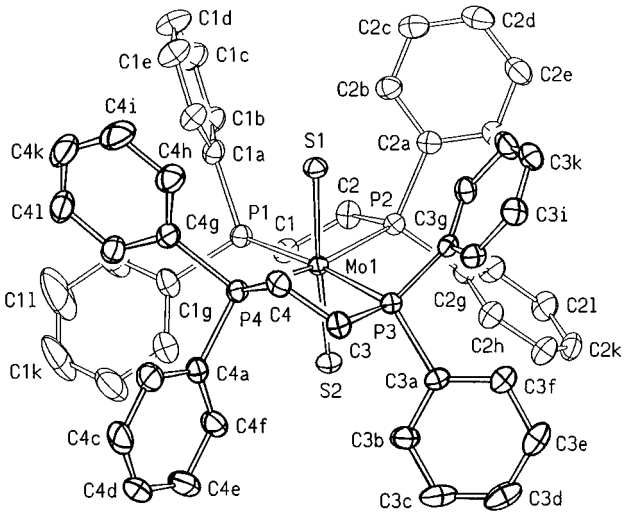

Figure 8. Molecular structure representation and atom-numbering scheme of *trans*-Mo(S)$_2$(dppe)$_2$ (**5**). The crystal structure of *trans*-Mo(Se)$_2$(dppe)$_2$ (**6**) is isomorphous with that of **5**. The same numbering system was used for **6**.

Table 4. Selected Bond Lengths (Å) and Angles (deg) for *trans*-Mo(S)$_2$(dppee)$_2$ (**2**)[a]

Mo(1)−S(1)	2.2280(14)		
Mo(1)−P(1)	2.5098(10)	Mo(1)−P(2)	2.5007(11)
P(1)−C(1)	1.826(3)	P(2)−C(2)	1.825(3)
P(1)−C(1a)	1.836(3)	P(2)−C(2a)	1.826(3)
P(1)−C(1g)	1.833(3)	P(2)−C(2g)	1.831(3)
C(1)−C(2)	1.308(4)		
S(1)−Mo(1)−P(1)	89.14(5)	S(1)−Mo(1)−P(2)	88.54(4)
S(1)−Mo(1)−P(1)^i	90.86(5)	S(1)−Mo(1)−P(2)^i	91.46(4)
P(1)−Mo(1)−P(2)	81.04(3)	P(1)−Mo(1)−P(2)^i	98.96(3)
C(1)−P(1)−C(1a)	100.46(13)	C(2)−P(2)−C(2a)	100.99(13)
C(1)−P(1)−C(1g)	100.48(13)	C(2)−P(2)−C(2g)	99.90(13)
C(1a)−P(1)−C(1g)	100.81(14)	C(2a)−P(2)−C(2g)	100.91(13)
P(1)−C(1)−C(2)	122.3(2)	P(2)−C(2)−C(1)	122.2(2)

[a] Symmetry transformation used to generate equivalent atoms: (i) $-x, -y, -z$.

the corresponding average bond angles and distances are 2.254(1) Å and 179.4(2)°.[14] The Mo═S bond lengths are again completely independent of the nature of the equatorial ligands. Even the slight differences in the Mo═S bond lengths in **5** (2.236(1) and 2.249(1) Å) are reflected (2.232(9) and 2.245(8) Å) in the crown thioether complex *trans*-Mo(S)$_2$(*syn*-Me$_8$[16]aneS$_4$)$_2$.[15]

These *pure* Mo═S double bonds are significantly longer than those in complexes where the sulfur atom either is in a terminal position or has a cis configuration due to the missing triple-bond contribution. This type of bond length falls into the narrow range from about 2.11 to 2.18 Å (for a detailed table, see ref 14). When one of the axial sulfur atoms is not a sulfido group (i.e., SMe), the bond order between the metal and that sulfur decreases to about 1 (Mo−SMe = 2.440(6) Å), whereas the bond order of the atom trans to it formally increases to 3 (Mo≡S = 2.140(5) Å) (Figure 9).[21]

The higher congeners of complexes **2** and **5** are the selenium complexes *trans*-Mo(Se)$_2$(dppee)$_2$ (**3**) and *trans*-Mo(Se)$_2$(dppe)$_2$ (**6**). **3** crystallizes in the space group $P2_1/c$ residing on a crystallographic inversion center (Figure 10), and **6** is isostructural with **5**. Structurally, the main difference between **6** and **5** is the longer Mo═Q bond length. The atom-numbering system is identical to the one used for **5**. No extra figure was introduced

(21) Yoshida, T.; Adachi, T.; Matsumura, K.; Baba, K. *Chem. Lett.* **1992**, 2447.

Table 5. Selected Bond Lengths (Å) and Angles (deg) for *trans*-Mo(S)$_2$(dppe)$_2$ (**5**)·$^1/_2$C$_7$H$_8$

Mo(1)−S(1)	2.2356(11)	Mo(1)−S(2)	2.2488(11)
Mo(1)−P(1)	2.5197(11)	Mo(1)−P(2)	2.5371(11)
Mo(1)−P(3)	2.5488(11)	Mo(1)−P(4)	2.5097(12)
P(1)−C(1)	1.825(5)	P(2)−C(2)	1.855(4)
P(1)−C(1a)	1.831(4)	P(2)−C(2a)	1.839(4)
P(1)−C(1g)	1.827(4)	P(2)−C(2g)	1.838(4)
P(3)−C(3)	1.865(4)	P(4)−C(4)	1.837(5)
P(3)−C(3a)	1.844(4)	P(4)−C(4a)	1.843(5)
P(3)−C(3g)	1.833(4)	P(4)−C(4g)	1.826(4)
C(1)−C(2)	1.506(6)	C(3)−C(4)	1.513(7)
S(1)−Mo(1)−S(2)	175.51(4)		
S(1)−Mo(1)−P(1)	95.34(4)	S(2)−Mo(1)−P(1)	86.58(4)
S(1)−Mo(1)−P(2)	91.44(4)	S(2)−Mo(1)−P(2)	84.93(4)
S(1)−Mo(1)−P(3)	87.59(4)	S(2)−Mo(1)−P(3)	90.74(4)
S(1)−Mo(1)−P(4)	82.12(4)	S(2)−Mo(1)−P(4)	101.68(4)
P(1)−Mo(1)−P(2)	78.77(4)	P(1)−Mo(1)−P(3)	175.47(4)
P(1)−Mo(1)−P(4)	97.60(4)	P(2)−Mo(1)−P(3)	104.65(4)
P(2)−Mo(1)−P(4)	172.33(4)	P(3)−Mo(1)−P(4)	79.35(4)
C(1)−P(1)−C(1a)	103.1(2)	C(2)−P(2)−C(2a)	100.8(2)
C(1)−P(1)−C(1g)	101.4(2)	C(2)−P(2)−C(2g)	103.1(2)
C(1a)−P(1)−C(1g)	102.6(2)	C(2a)−P(2)−C(2g)	102.0(2)
P(1)−C(1)−C(2)	110.9(3)	P(2)−C(2)−C(1)	113.9(3)
C(3)−P(3)−C(3a)	99.1(2)	C(4)−P(4)−C(4a)	100.2(2)
C(3)−P(3)−C(3g)	102.7(2)	C(4)−P(4)−C(4g)	104.8(2)
C(3a)−P(3)−C(3g)	103.3(2)	C(4a)−P(4)−C(4g)	100.7(2)
P(3)−C(3)−C(4)	111.8(3	P(4)−C(4)−C(3)	108.8(3)

Table 6. Selected Bond Lengths (Å) and Angles (deg) for *trans*-Mo(Se)$_2$(dppee)$_2$ (**3**)·CH$_2$Cl$_2$[a]

Mo(1)−Se(1)	2.356(2)		
Mo(1)−P(1)	2.514(2)	Mo(1)−P(2)	2.503(2)
P(1)−C(1)	1.834(9)	P(2)−C(2)	1.826(8)
P(1)−C(1a)	1.835(9)	P(2)−C(2a)	1.838(8)
P(1)−C(1g)	1.837(8)	P(2)−C(2g)	1.820(9)
C(1)−C(2)	1.337(12)		
Se(1)−Mo(1)−P(1)	88.56(7)	Se(1)−Mo(1)−P(2)	88.12(6)
Se(1)−Mo(1)−P(1)^i	91.45(7)	Se(1)−Mo(1)−P(2)^i	91.88(6)
P(2)−Mo(1)−P(1)	79.71(7)	P(2)−Mo(1)−P(1)^i	100.29(7)
C(1)−P(1)−C(1a)	101.4(4)	C(2)−P(2)−C(2a)	102.0(4)
C(1)−P(1)−C(1g)	99.4(4)	C(2)−P(2)−C(2g)	98.7(4)
C(1a)−P(1)−C(1g)	100.8(4)	C(2a)−P(2)−C(2g)	100.7(4)
P(1)−C(1)−C(2)	121.3(6)	P(2)−C(2)−C(1)	120.5(7)

[a] Symmetry transformation used to generate equivalent atoms: (i) $-x, -y, -z$.

because the ORTEP drawings of **6** and **5** appear almost identical (Figure 8). The positional and isotropic equivalent temperature parameters of **3** and **6** are listed in Tables 9 and 11, respectively, and selected bond distances and angles for these compounds are summarized in Tables 10 and 12, respectively.

In **3** and **6**, the Mo═Se bond distances and the Se═Mo═Se bond angles are respectively 2.356(1) Å, 180° and 2.377(1) Å, 2.386(1) Å, 174.65(5)°. In the PMe$_3$ analog, the Mo═Se bond length (average 2.383(2) Å) is almost identical to the values found in **3** and **6**.[14] Among the three complexes discussed, the greatest deviation in the Se═Mo═Se angle from 180° was observed in **6** (5.35(5)°). The interpretation of the bond lengths proceeds exactly as for the sulfur homologs. "Pure" double bonds fall into a range of about 2.37−2.39 Å and are significantly longer than double bonds with a triple-bond contribution (2.24−2.30 Å[14]).

The heaviest congener of the series *trans*-Mo(Q)$_2$(dppee)$_2$ is *trans*-Mo(Te)$_2$(dppee)$_2$ (**4**). **4** crystallizes in the space group $P\bar{1}$ with two independent half-molecules found in the asymmetric unit. Each of them is completed by inversion at two different centers of $P\bar{1}$. In Figure 11, only one arbitrary molecule of **4** was chosen.

The Mo═Te bond distances are 2.562(1) Å in **4(1)** and 2.557(1) Å in **4(2)**. These are slightly shorter than those in *trans*-

Table 7. Selected Bond Lengths (Å) and Angles (deg) for *trans*-Mo(Se)$_2$(dppe)$_2$ (**6**)·$^1/_2$C$_7$H$_8$

Mo(1)−Se(1)	2.3774(13)	Mo(1)−Se(2)	2.3860(13)
Mo(1)−P(1)	2.516(2)	Mo(1)−P(2)	2.530(2)
Mo(1)−P(3)	2.545(2)	Mo(1)−P(4)	2.509(2)
P(1)−C(1)	1.829(9)	P(2)−C(2)	1.856(8)
P(1)−C(1a)	1.840(9)	P(2)−C(2a)	1.845(9)
P(1)−C(1g)	1.839(9)	P(2)−C(2g)	1.840(8)
P(3)−C(3)	1.869(9)	P(4)−C(4)	1.841(9)
P(3)−C(3a)	1.844(9)	P(4)−C(4a)	1.833(9)
P(3)−C(3g)	1.826(9)	P(4)−C(4g)	1.823(9)
C(1)−C(2)	1.494(13)	C(3)−C(4)	1.499(13)
Se(1)−Mo(1)−Se(2)	174.65(5)		
Se(1)−Mo(1)−P(1)	95.69(6)	Se(2)−Mo(1)−P(1)	86.87(6)
Se(1)−Mo(1)−P(2)	91.16(6)	Se(2)−Mo(1)−P(2)	84.74(6)
Se(1)−Mo(1)−P(3)	87.18(6)	Se(2)−Mo(1)−P(3)	90.55(6)
Se(1)−Mo(1)−P(4)	82.05(6)	Se(2)−Mo(1)−P(4)	102.28(6)
P(1)−Mo(1)−P(2)	78.39(7)	P(1)−Mo(1)−P(3)	175.56(8)
P(1)−Mo(1)−P(4)	97.92(8)	P(2)−Mo(1)−P(3)	104.98(7)
P(2)−Mo(1)−P(4)	171.97(8)	P(3)−Mo(1)−P(4)	79.10(8)
P(1)−C(1)−C(2)	110.3(6)	P(2)−C(2)−C(1)	114.0(6)
C(1)−P(1)−C(1a)	103.2(4)	C(2)−P(2)−C(2g)	102.5(4)
C(1)−P(1)−C(1g)	101.2(4)	C(2)−P(2)−C(2a)	101.2(4)
C(1a)−P(1)−C(1g)	102.5(4)	C(2g)−P(2)−C(2a)	101.6(4)
P(3)−C(3)−C(4)	111.4(6)	P(4)−C(4)−C(3)	109.0(6)
C(3)−P(3)−C(3a)	99.2(4)	C(4)−P(4)−C(4a)	100.4(4)
C(3)−P(3)−C(3g)	102.8(4)	C(4)−P(4)−C(4g)	105.1(4)
C(3a)−P(3)−C(3g)	102.7(4)	C(4a)−P(4)−C(4g)	99.9(4)

Table 8. Selected Bond Lengths (Å) and Angles (deg) for *trans*-Mo(Te)$_2$(dppee)$_2$ (**4**)[a]

Mo(1)−Te(1)	2.5615(10)		
Mo(1)−P(11)	2.520(3)	Mo(1)−P(12)	2.513(2)
P(11)−C(11)	1.819(10)	P(12)−C(12)	1.823(10)
P(11)−C(11a)	1.843(10)	P(12)−C(12a)	1.844(11)
P(11)−C(11g)	1.825(11)	P(12)−C(12g)	1.832(10)
C(11)−C(12)	1.311(14)		
Te(1)−Mo(1)−P(11)	92.77(7)	Te(1)−Mo(1)−P(12)	93.53(6)
Te(1)−Mo(1)−P(11)^{i}	87.23(7)	Te(1)−Mo(1)−P(12)^{i}	86.47(6)
P(12)−Mo(1)−P(11)	80.35(9)	P(12)−Mo(1)−P(11)^{i}	99.65(9)
C(11)−P(11)−C(11a)	101.0(5)	C(12)−P(12)−C(12a)	96.8(5)
C(11)−P(11)−C(11g)	97.3(5)	C(12)−P(12)−C(12g)	102.1(5)
C(11a)−P(11)−C(11g)	101.0(5)	C(12a)−P(12)−C(12g)	99.4(5)
P(11)−C(11)−C(12)	122.1(8)	P(12)−C(12)−C(11)	122.1(7)
Mo(2)−Te(2)	2.5566(11)		
Mo(2)−P(21)	2.510(3)	Mo(2)−P(22)	2.519(3)
P(21)−C(21)	1.836(10)	P(22)−C(22)	1.791(11)
P(21)−C(21a)	1.827(11)	P(22)−C(22a)	1.864(10)
P(21)−C(21g)	1.826(10)	P(22)−C(22g)	1.837(11)
C(21)−C(22)	1.32(2)		
Te(2)−Mo(2)−P(21)^{ii}	91.62(6)	Te(2)−Mo(2)−P(22)^{ii}	92.80(7)
Te(2)−Mo(2)−P(21)	88.38(6)	Te(2)−Mo(2)−P(22)	87.20(7)
P(22)−Mo(2)−P(21)	79.46(9)	P(22)−Mo(2)−P(21)^{ii}	100.54(9)
C(21)−P(21)−C(21a)	98.5(5)	C(22)−P(22)−C(22a)	98.7(5)
C(21)−P(21)−C(21g)	101.4(5)	C(22)−P(22)−C(22g)	103.5(5)
C(21a)−P(21)−C(21g)	99.8(4)	C(22a)−P(22)−C(22g)	101.8(5)
P(21)−C(21)−C(22)	119.9(9)	P(22)−C(22)−C(21)	123.3(9)

[a] Symmetry transformations used to generate equivalent atoms: (i) $-x, -y + 1, -z$; (ii) $-x, -y, -z$.

Mo(Te)$_2$(PMe$_3$)$_4$ (2.597(1) Å).[14] The Mo═Q bond lengths in the series *trans*-Mo(Q)$_2$(dppee)$_2$ (Q = O, S, Se, Te) increase uniformly with an increase of the covalent radii of Q. This is particularly noticeable if Q = O is excluded (sum of covalent radii [Å],[22] bond length for P⁀P = dppee [Å], difference [Å]: Q = O, 2.03, 1.804(2), 0.23; Q = S, 2.32, 2.228(1), 0.09; Q = Se, 2.46, 2.356(2), 0.10; Q = Te, 2.66, average 2.559(2), 0.10). The larger difference between the sum of covalent radii and observed bond length when Q = O might be due the higher donor ability of the oxygen ligand in comparison to the other chalcogens.

(22) *Table of Periodic Properties of the Elements*; Sargent-Welch Scientific Co.: 1980; Catalog No. S-18806.

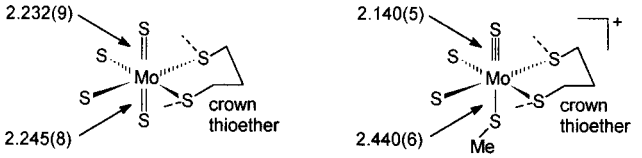

Figure 9. Changes in the bond order upon alkyation of one sulfur atom. The formal bond order is illustarted in valence bond line notation (data used were from refs 15 and 21).

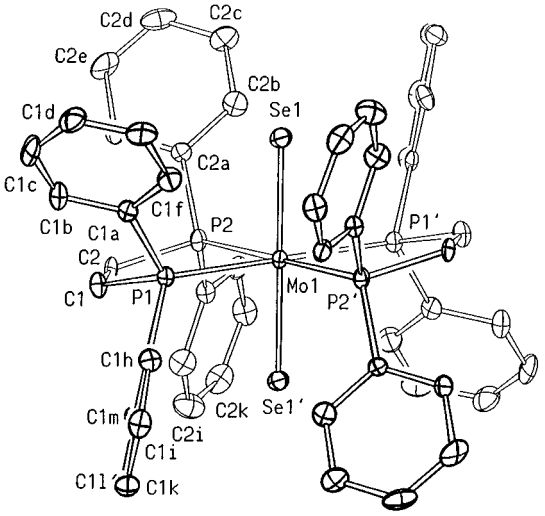

Figure 10. Molecular structure representation and atom-numbering scheme of *trans*-Mo(Se)$_2$(dppee)$_2$ (**3**).

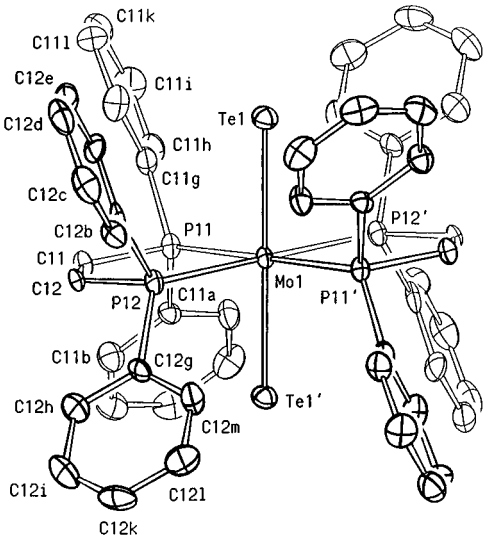

Figure 11. Molecular structure representation and atom-numbering scheme of *trans*-Mo(Te)$_2$(dppee)$_2$ (**4**).

In **1**−**6**, the competitive interaction between the two chalcogens in the axial positions is equal on both sides. However, if the two chalcogen atoms differ in their donor ability, some effect on the bond lengths should be seen. We determined the structure of *trans*-Mo(O)(S)(dppee)$_2$ (**7**) (Figure 12; selected bond lengths and angles are given in Table 9). **7** resides on a crystallographic inversion center which introduces a disorder in the S and O atoms in the ratio 1:1. This model was successfully used in the refinement.

The Mo═S and Mo═O bond lengths were determined to be 2.244(3) and 1.843(6) Å, respectively. The O═Mo═S bond

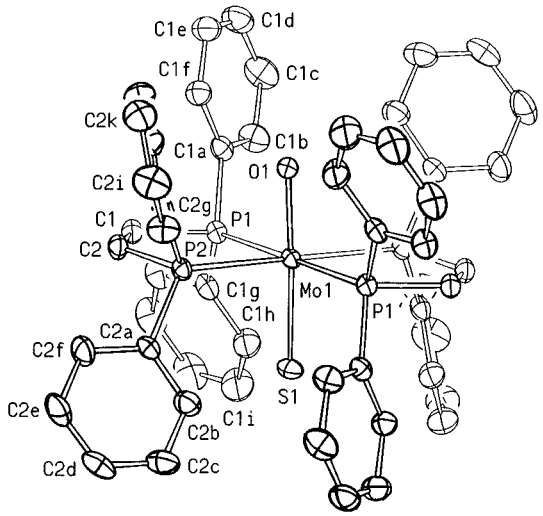

Figure 12. Molecular structure representation and atom-numbering scheme of *trans*-Mo(O)(S)(dppee)$_2$ (**7**).

Table 9. Selected Bond Lengths (Å) and Angles (deg) for *trans*-Mo(O)(S)(dppee)$_2$ (**7**)[a]

Mo(1)−O(1)	1.843(6)	Mo(1)−S(1)	2.244(3)
Mo(1)−P(1)	2.5061(8)	Mo(1)−P(2)	2.5125(8)
P(1)−C(1)	1.823(3)	P(2)−C(2)	1.824(3)
P(1)−C(1a)	1.827(3)	P(2)−C(2a)	1.830(3)
P(1)−C(1g)	1.834(3)	P(2)−C(2g)	1.835(3)
C(1)−C(2)	1.318(4)		
O(1)−Mo(1)−S(1)	176.8(2)		
O(1)−Mo(1)−P(1)	93.8(2)	O(1)−Mo(1)−P(1)^{i}	86.2(2)
O(1)−Mo(1)−P(2)	92.7(2)	O(1)−Mo(1)−P(2)^{i}	87.3(2)
S(1)−Mo(1)−P(1)	89.15(6)	S(1)−Mo(1)−P(1)^{i}	90.85(6)
S(1)−Mo(1)−P(2)	88.79(6)	S(1)−Mo(1)−P(2)^{i}	91.21(6)
P(1)−Mo(1)−P(2)	80.76(3)	P(1)−Mo(1)−P(2)^{i}	99.24(2)
C(1)−P(1)−C(1a)	100.82(14)	C(2)−P(2)−C(2a)	101.22(14)
C(1)−P(1)−C(1g)	100.10(14)	C(2)−P(2)−C(2g)	100.67(14)
C(1a)−P(1)−C(1g)	102.84(14)	C(2a)−P(2)−C(2g)	101.71(14)
P(1)−C(1)−C(2)	121.9(2)	P(2)−C(2)−C(1)	122.2(2)

[a] Symmetry transformation used to generate equivalent atoms: (i) $-x+1, -y+1, -z+1$.

angle is 176.8(2)°. These values fit almost perfectly to the Mo═Q bond lengths found in **1** (1.804 (2) Å) and **2** (2.228(1) Å). However, upon comparison with the only other example of a *trans*-Mo(O)(S)(P⁀P)$_2$ type structure, *trans*-Mo(O)(S)-(dppe)$_2$,[16] we find some rather large differences (2.415(7), 1.77-(1) Å). Initially, some doubts arose regarding the reliability of this structural determination because SO_2, H_2SO_4, toluene, and ethanol were found in the lattice. Therefore, the alternative formulation [*trans*-Mo(O)(SH)(dppe)$_2$]$^+$[HSO_4^-] comes into consideration,[14] and all differences in the bond lengths could be explained by this alternative. For this reason, further examination of this structure is warranted. A closer look at the published atomic coordinates reveals possible locations for the protons. The authors of ref 16 claimed that they found two short S═O and two long S−OH bond lengths in the H_2SO_4 molecule. This seems to be true only at first glance. The two longer S−O bonds belong to a hydrogen-bridged dimerization across a crystallographic inversion center such as often occurs in the structures of carboxylic acids (O(21)···O(23) = 2.56(3) Å). This hydrogen bridge accounts only for *one* proton. We found another short contact between O(22) and S(3) of the SO_2 molecule (2.48(2) Å), which leads to a second possible location for a proton (Figure 13). Of course, disorder among the positions is possible. The S−O bond lengths (average 1.37(4) Å) are shorter than expected for SO_2 (1.4321 Å[23]), but this could

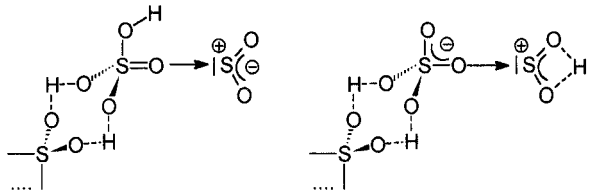

Figure 13. Possible locations of protons in a H_2SO_4/SO_2 network.

of course be due to the very high temperature parameter of these atoms. In light of these considerations it would seem that the authors of ref 16 correctly formulated the compound.

How, then, do we account for the fact that the Mo═O and the Mo═S bond lengths in **7** appear to be too long and too short, respectively. The separation between the disordered O(1) and S(1) is 0.401(6) Å, which is far below the resolution of the X-ray experiment (Cu Kα; $\theta_{max} = 120°$, $\lambda/(2 \sin\theta) = 0.89$ Å). Maxima of two overlapping functions will move together if the separation/resolution is not large enough (i.e., if the maxima are not sufficiently sharp). Luckily, in this laboratory, we have determined the structure of the cation *trans*-Mo(O)(Cl)(dppee)$_2^+$ first in a perfectly ordered structure and then in a crystal exhibiting the same disorder problem.[24] The scattering powers of S and Cl differ by only one electron, and the length of the Mo−Cl bond is very similar to that for an Mo−S bond. In the disordered case, the average Mo═O and the Mo−Cl bond lengths appeared to be 1.842(8) and 2.296(7) Å whereas the real values are 1.684(3) and 2.434(2) Å (differences: 0.158 and 0.138 Å!).

Additional support for a very short Mo−O bond and a longer Mo−S bond is provided by the chemistry of related compounds. We saw that the nature of the equatorial ligands has only minor effects on the bond lengths of the axial ligands. The cationic complex *trans*-Mo(O)(SH)(*syn*-[16]aneS$_4$)$_2^+$ exhibits Mo≡O and Mo−SH bond lengths of 1.667(3) and 2.484(2) Å.[25] In this case, the bond orders are certain and are as shown by the valence line notation. Since the Mo to O bond lengths are significantly longer in **7** or *trans*-Mo(O)(S)(dppe)$_2$ than in *trans*-Mo(O)(SH)(*syn*-[16]aneS$_4$)$_2^+$, the axial moiety of **7** and *trans*-Mo(O)(S)(dppe)$_2$ should be formulated as

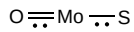

The stronger donor O forms a bond stronger than the "pure" double bond and the S atom forms a bond weaker than the "pure" double bond to Mo.

Because of the crystallographic inversion center in complexes **1**−**4** and **7**, the equatorial phosphorus atoms form a perfect plane with Mo in the center. The bridging carbon atoms are distorted out of this plane, one dppee ligand lying above and the other one below the plane. The degree of bending varies among structures **1**−**4** and **7** due to packing forces (minimum average 0.072(3) Å in **2**, maximum average 0.367(9) Å in **3**, i.e. 0.054-(10) Å in **4(1)** and 0.123(11) Å in **4(2)**). No contacts between the double bond of the ethylene bridge and the Mo atom were observed. The equatorial plane of complexes **5** and **6** is much more distorted. P(1) (**5**, 0.112(1) Å; **6**, 0.115(1) Å) is located above, P(2) (0.105(1), 0.108(1) Å) below, P(3) (0.104(1), 0.107-(1) Å) above, and P(4) (0.111(1), 0.114(1) Å) below the least-squares plane. The chelating dppe ligands are distorted, and

(23) Weast, R. C., Astle, M. J., Beyer, W. H., Eds. *CRC Handbook of Chemistry and Physics*, 66th ed.; CRC: Boca Raton, FL, 1985; p F-167.
(24) Cotton, F. A.; Mandel, S. J.; Schmid, G. Unpublished results.
(25) DeSimone, R. E.; Glick, M. D. *Inorg. Chem.* **1978**, *17*, 3574.

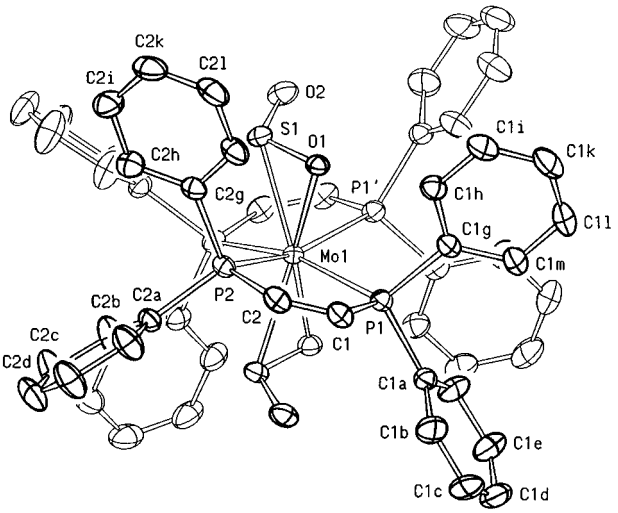

Figure 14. Molecular structure representation and atom-numbering scheme of $Mo(SO_2)_2(dppee)_2$ (**8**). The 2-fold axis which bisects the molecular structure lies approximately in the *x* direction of the paper plane going through Mo(1).

Table 10. Selected Bond Lengths (Å) and Angles (deg) for $Mo(SO_2)_2(dppee)_2$ (**8**)[a]

Mo(1)−S(1)	2.4394(9)	Mo(1)−O(1)	2.115(2)
Mo(1)−P(1)	2.5573(7)	Mo(1)−P(2)	2.5239(8)
S(1)−O(2)	1.469(2)	S(1)−O(1)	1.564(2)
P(1)−C(1)	1.814(3)	P(2)−C(2)	1.817(3)
P(1)−C(1a)	1.827(3)	P(2)−C(2a)	1.834(3)
P(1)−C(1g)	1.844(3)	P(2)−C(2g)	1.840(3)
C(1)−C(2)	1.306(4)		
O(1)−Mo(1)−O(1)^{i}	157.54(10)	S(1)−Mo(1)−S(1)^{i}	146.29(4)
O(1)−Mo(1)−P(1)	85.60(5)	O(1)−Mo(1)−P(1)^{i}	79.63(5)
O(1)−Mo(1)−P(2)	115.96(5)	O(1)−Mo(1)−P(2)^{i}	78.07(5)
O(1)−Mo(1)−S(1)	39.35(5)	O(1)−Mo(1)−S(1)^{i}	152.40(5)
S(1)−Mo(1)−P(1)	84.25(3)	S(1)−Mo(1)−P(1)^{i}	118.84(3)
S(1)−Mo(1)−P(2)	77.11(3)	S(1)−Mo(1)−P(2)^{i}	83.06(3)
O(1)−S(1)−Mo(1)	59.06(7)	O(2)−S(1)−Mo(1)	114.40(9)
O(2)−S(1)−O(1)	113.61(12)		
P(1)−Mo(1)−P(1)^{i}	97.55(3)	P(2)−Mo(1)−P(2)^{i}	107.27(4)
P(2)−Mo(1)−P(1)	79.74(3)	P(2)−Mo(1)−P(1)^{i}	163.67(2)
C(1)−P(1)−C(1a)	104.18(14)	C(2)−P(2)−C(2a)	102.25(13)
C(1)−P(1)−C(1g)	97.76(13)	C(2)−P(2)−C(2g)	99.84(14)
C(1a)−P(1)−C(1g)	101.50(13)	C(2a)−P(2)−C(2g)	99.95(13)
P(1)−C(1)−P(2)	121.9(2)	P(2)−C(2)−C(1)	123.1(2)

[a] Symmetry transformation used to generate equivalent atoms: (i) $-x + 1, y, -z + 3/2$.

the Q═Mo═Q bond angles differ slightly from 180° (**5**, 4.49(4)°; **6**, 5.35(5)°) due to packing forces. In **1**−**4** and **7**, the Mo−P bond lengths vary in the small range from 2.501(1) to 2.520(3) Å, the average value being 2.510(6) Å. In **5** and **6**, the range was found to be from 2.509(2) to 2.549(1) Å (average 2.527(15) Å). The Mo−P bond lengths agree very well with those exhibited by *trans*-$Mo(Q)_2(PMe_3)_4$ (average 2.518(4) Å; Q = S, Se, Te[14]) or *trans*-Mo(O)(S)$(dppe)_2$ (average 2.557(8) Å[16]). The intraligand P−Mo−P bond angles are dominated by the geometry of the dppee or dppe ligand, ranging from 79.46(9) to 81.04(3)° for dppee and from 78.39(7) to 79.35(4)° for dppe. All Q═Mo−P bond angles are in the expected range, from about 80 to 90°. The phenyl substituents of the P P ligands are planar within the experimental error.

$Mo(SO_2)_2(dppee)_2$ (**8**) was obtained in the attempted preparation of **7**. **8** crystallizes in the space group *C*2/*c*, residing on a crystallographic 2-fold axis (Figure 14). The selected bond distances and angles of **8** are summarized in Table 10.

The geometry of the 8-coordinate complex **8** can still be discussed as a distorted octahedron. The base is formed by the P atoms of the dppee ligands, with the Mo atom in the center. It is distorted in such a manner that P(1) (0.354 Å) lies below and P(2) (0.334 Å) above the least-squares plane of the 4 P atoms. The other half of the molecule is created by the 2-fold axis. At the apex positions, SO_2 molecules are coordinated in an η^2-fashion. SO_2 can coordinate in a number of different ways, but we want to discuss here only the way that is found in **8**.[26] In this Mo(0) complex, the Mo(1)−S(1) and the Mo(1)−O(1) bond lengths are 2.439(1) and 2.115(2) Å, respectively. Both values fall into the single-bond region, which was discussed for the Mo(IV) complexes **1**−**7**. The S(1)−O(1) bond length, at 1.564(2) Å, is significantly elongated when compared to that in an uncoordinated SO_2 molecule (1.4321 Å).[23] The S(1)−O(2) bond length remains shorter, at 1.469(2) Å. The O(1)−S(1)−O(2) bond angle of 113.61(12)° is slightly less obtuse than that found in the uncoordinated SO_2 molecule (119.54°). A few Mo compounds where the SO_2 molecule is η^2-coordinated were previously prepared. A comparison of the η^2-SO_2 moiety in **8** with those in the complexes $Mo(CO)_2(bpy)(SO_2)_2$ (bpy = bipyridyl),[27] $Mo(CO)_3(phen)(SO_2)$ (phen = phenanthroline),[27] $Mo(S_2CNEt_2)(SO_2)$,[28] and $Mo(CO)_2(PMe_3)_3(SO_2)$[29] is presented in Table 11.

Table 11. Comparison of Structures Containing the Mo(η^2-SO_2) Unit (Distances, Å; Angles, deg)

	8	*a*	*b*	*c*	*d*
Mo−S	2.439(1)	av 2.496(2)	2.532(3)	2.463(4)	2.470(1)
Mo−O	2.115(2)	av 2.111(4)	2.223(5)	2.149(8)	2.186(3)
S−O	1.564(2)	av 1.550(6)	1.468(5)	1.506(9)	1.542(3)
S═O	1.469(2)	av 1.453(5)	1.434(8)	1.440(11)	1.477(3)
S−Mo−O	39.35(5)			37.3(2)	38.06(7)
O−S═O	113.6(1)	av 113.4(3)	117.3(4)	114.5(6)	113.0(2)

[a] $Mo(CO)_2(bpy)(SO_2)_2$.[27] [b] $Mo(CO)_3(phen)(SO_2)$.[27] [c] $Mo(S_2CNEt_2)(SO_2)$.[28] [d] $Mo(CO)_2(PMe_3)_3(SO_2)$.[29]

The Mo−P bond lengths in **8** are at the upper limit of the range seen in **1**−**4** and **7** (2.557(1), 2.524(1) Å). The reason might be the lower oxidation state of the Mo atom in **8**. All phenyl groups are planar within the experimental error. The overall geometry of the dppee ligand is as expected.

UV/Vis Spectroscopy. The UV/vis spectra were recorded for solutions which were first checked for purity by $^{31}P\{^{1}H\}$ NMR. A summary of the bands found is given in Table 12, where the intensity of the band with the highest absorption was arbitrarily set to 100. The extinction coefficients were not quantified because of the low solubilities of the complexes. In Figures 15 (**1**−**4**) and 16 (**5**, **6**), the spectra are compiled to show the main features.

The spectra can be divided into four sections: first the region before the band with the highest absorption, second the dominating band, third the region just after the dominating band, and fourth the very weak bands in the low-energy region. The dominating band is significantly shifted to lower energy in the spectra of complexes **2** (374 nm), **3** (414 nm), and **4** (485 nm) as the chalcogen atoms progress from S to Se to Te. This band moves slightly to lower energy upon increasing the basicity of the phosphine ligand (Q = S: **2**, 374 nm; **5**, 380 nm. Q = Se: **3**, 414 nm; **6**, 420 nm; *trans*-$Mo(Se)_2(PMe_3)_4$, 424 nm.[14] Q = Te: **4**, 485 nm; *trans*-$Mo(Te)_2(PMe_3)_4$, 488 nm[14]). Very weak bands were found in the low-energy region between 547 nm

(26) Ryan, R. R.; Kubas, G. J.; Moddy, D. C.; Eller, P. G. *Struct. Bonding* **1981**, *46*, 47.
(27) Kubas, G. J.; Ryan, R. R.; McCarty, V. *Inorg. Chem.* **1980**, *19*, 3003.
(28) Broomhead, J. A.; Gill, N. S.; Hammer, B. C.; Sterns, M. *J. Chem. Soc., Chem. Commun.* **1982**, 1234.
(29) Baumann, F.-E.; Burschka, C.; Schenk, W. A. *Z. Naturforsch.* **1986**, *41B*, 1211.

Table 12. UV/Vis Data for the Complexes **1**−**6**[a]

1		373 (sh, 100)	438 (25)		pale yellow	light yellow
2	319 (51)	374 (100)	414 (sh, 10), 433 (sh, 6)	547 (0.5)	yellow	brown
3	322 (35)	414 (100)	520 (3)	585 (0.3), 637 (sh, 0.2)	yellow	green
4	320 (sh, 39), 352 (sh, 29), 386 (sh, 20)	485 (100)	624 (22)	773 (0.4), 807 (sh, 0.2)	green	dark green
5	320 (sh, 51), 340 (57)	380 (100)	431 (sh, 8)	547 (0.6)	green	dark green
6	320 (sh, 59) 343 (sh, 52)	420 (100)	514(4)	598 (0.3)	yellow	brown

[a] In the last two columns the colors of the solutions and the colors of the crystals are listed. The intensity of the band with the highest absorption was arbitrarily set to 100.

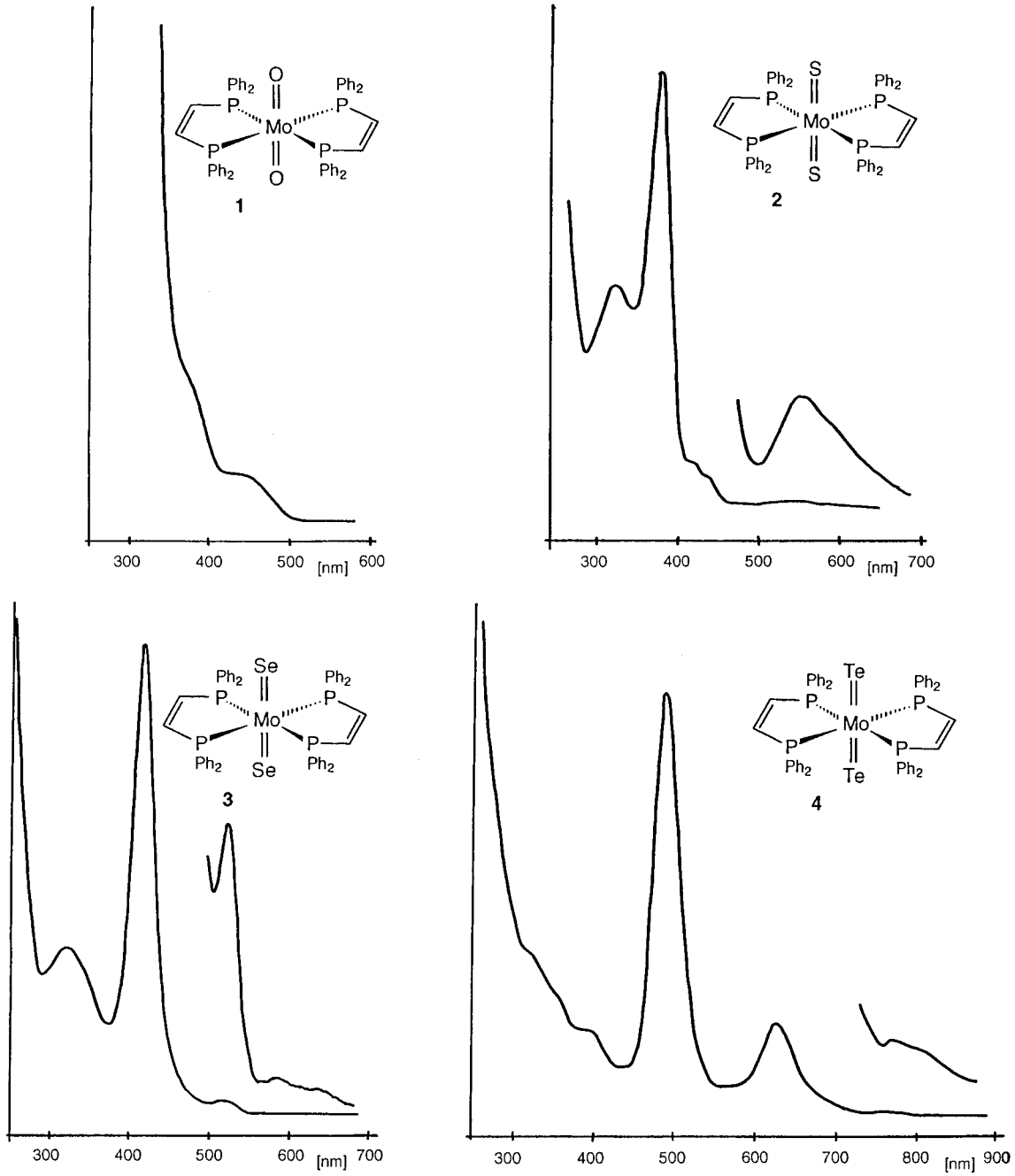

Figure 15. UV/vis spectra of complexes **1**−**4**. The extinction coefficients were not quantified.

(**2**), 585, 637 nm (**3**) and 773, 807 nm (**4**) for P⌒P = dppee and between 547 nm (**5**) and 598 nm (**6**) for P⌒P = dppe.

The electronic structure of these compounds might be predicted on the basis of ligand field theory including metal−ligand π interactions. The results of SCF−Xα−SW molecular orbital calculations are in full agreement with such a prediction. According to the calculations, the lowest energy band should be assigned to a nonbonding $d_{xy} \rightarrow \pi^*$ excitation. But the role of the lone pair orbitals of the chalcogen atoms (e_{1u} symmetry) changes when *ab initio* methods are used. The lowest absorption band should be assigned to transitions corresponding to ligand to metal charge transfer (LMCT) rather than metal-based d−d transitions. A detailed discussion can be found in the earlier theoretical paper.[3]

The spectrum of **1** differs remarkably from all others in the series (Figure 15). Only a weak band at 438 nm and a shoulder

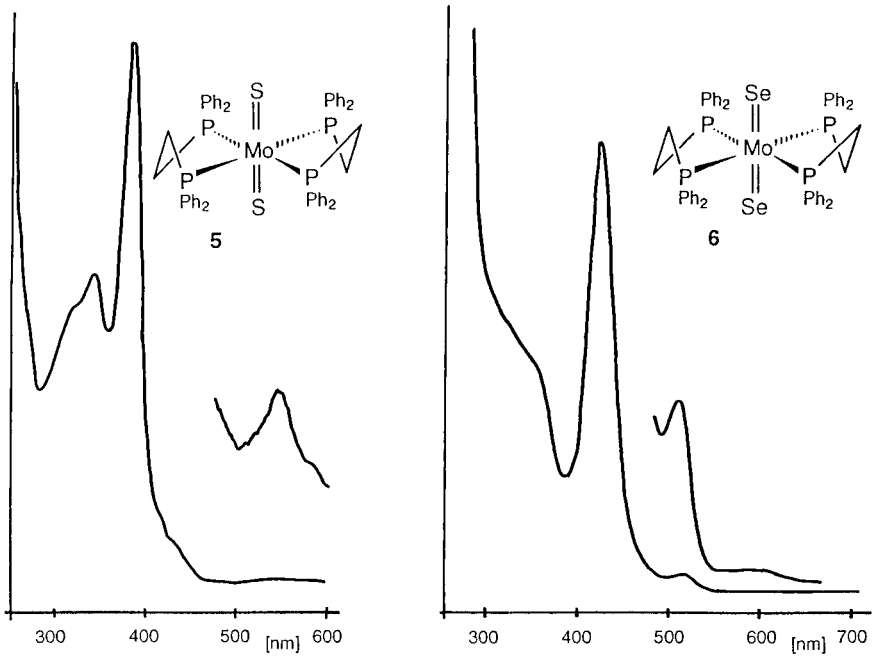

Figure 16. UV/vis spectra of complexes **5** and **6**. The extinction coefficients were not quantified.

at 373 nm were observed. These transitions were assigned to the singlet and triplet components of the $d_{xy} \rightarrow d_{x^2-y^2}$ excitation and were discussed in great detail previously.[3]

Conclusions

Complexes of the type *trans*-Mo(Q)$_2$(P⁀P)$_2$ where Q = S, Se, or Te and P⁀P = dppee or dppe can be obtained by the reaction between the dinitrogen complexes Mo(N$_2$)$_2$(P⁀P)$_2$ and a chalcogen source. The oxygen analog was prepared by hydrolysis of *trans*-Mo(O)(Cl)(dppee)$_2^+$ with OH$^-$ and subsequent deprotonation. X-ray analysis of the octahedral complexes and their comparison with other complexes containing terminal chalcogen ligands reveal that the bond length of a "pure" Mo−Q double bond can be defined. If the complex contains two different chalcogen atoms (i.e., O and S), the oxygen has a stronger bonding tendency than sulfur. The transition from the double/double to the triple/single bonding state can be seen. The bonding in the equatorial *xy* plane affects the axial positions negligibly, as was shown by $^{31}P\{^1H\}$ NMR, UV/vis spectroscopy, and X-ray analyses.

Acknowledgment. We thank the National Science Foundation for support and the Alexander von Humboldt Foundation for a Feodor-Lynen Fellowship to G.S. We also thank Mr. A. Yokochi for help with the crystallography.

Supporting Information Available: Complete X-ray crystallographic files, in CIF format, are available. Access information is given on any current masthead page.

IC961071V